Mar Biol (2015) 162:2171–2186
DOI 10.1007/s00227-015-2753-2

ORIGINAL PAPER

Estimating zooplankton vertical distribution from combined LOPC and ZooScan observations on the Brazilian Coast

Catarina R. Marcolin[1] · **Rubens M. Lopes**[1] · **George A. Jackson**[2]

Received: 25 April 2015 / Accepted: 2 October 2015 / Published online: 14 October 2015

Abstract Although the technology for sampling zooplankton is rapidly evolving, it remains a challenge to determine species distributions with high spatial resolution. This study reports on a technique developed to estimate the mesozooplankton vertical distribution by combining the spatial resolution possible with laser optical particle counter (LOPC) profiles with the taxonomic resolution possible with vertically integrated zooplankton net samples. Data obtained from different coastal and oceanic ecosystems off Brazil were used for our analysis. The aggregate signals from LOPC data sets were removed, and the distributions of the residual *Zo*-particles, believed to describe zooplankton, were calculated. Significant correlations were then identified between the abundances of the *Zo*-particles in different size classes and the abundance and size distributions of zooplankton collected in a vertical integrated net sample and classified with a ZooScan system. A principal component analysis was carried out to identify and exclude outliers. After these procedures, multiple linear regression analyses were used to detect relationships among abundances of different zooplankton groups and multiple *Zo*-particle size classes. The resulting relationships were used to estimate the vertical distributions of the dominant zooplankton taxa—calanoids, poecilostomatoids, shrimp-like, and appendicularians—through the water column from the LOPC data. The results achieved the goal of estimating distributions of dominant zooplankton taxa with an improved spatial resolution. The analytical technique described here enabled the analysis of zooplankton vertical structure in a wide range of marine ecosystems off Brazil and could serve as a basis to revisit historical data collected with similar methods elsewhere.

Responsible Editor: X. Irigoyen.

Reviewed by E. Bachiller, D. Checkley, L. Guidi.

Electronic supplementary material The online version of this article (doi:10.1007/s00227-015-2753-2) contains supplementary material, which is available to authorized users.

✉ Catarina R. Marcolin
catmarcolin@gmail.com

Rubens M. Lopes
rubens@usp.br

George A. Jackson
gjackson@tamu.edu

[1] Oceanographic Institute, University of São Paulo, Praça do Oceanográfico 191, São Paulo 05508-120, Brazil

[2] Department of Oceanography, Texas A&M University; 3146 TAMU, College Station, TX 77843-3146, USA

Introduction

In face of the widespread concern about global warming, overfishing, pollution and other environmental impacts in the world's oceans, it is critical to understand how zooplankton organisms are distributed in space and time because of their pivotal importance in the aquatic food web (e.g., Calbet and Landry 2004) and biogeochemical cycles (e.g., Mitra et al. 2014). The spatial resolution of zooplankton sampling has significantly increased in the last two decades thanks to the development of optical systems for detecting and counting animals in their natural environment (Wiebe and Benfield 2003; Benfield et al. 2007). The laser optical particle counter (LOPC) and its predecessor, the OPC, are examples of widely applied instruments to estimate particle abundance and size with a high spatial resolution, as fine as at 1-m depth intervals. Several studies have used the LOPC to report on plankton

and particle distribution over large areas, particularly in the northern hemisphere (e.g., Basedow et al. 2010; Yamaguchi et al. 2014; Vandromme et al. 2014). Off Brazil and in many other tropical and subtropical areas, zooplankton abundance has usually been estimated from net-collected samples integrating the water column (Lopes 2007). Recent investigations have combined the LOPC and plankton nets to provide more comprehensive data on plankton and particle distributions (Schultes and Lopes 2009; Marcolin et al. 2013). Studies have shown that LOPC results compare well with data sets acquired with other sampling strategies, such as acoustics (Trudnowska et al. 2012), plankton-imaging instruments (Basedow et al. 2013), and plankton nets (Schultes and Lopes 2009), despite intrinsic limitations of each method.

Although the LOPC does not distinguish zooplankton from aggregates directly, methods have been developed to separate the two types of objects (Jackson and Checkley 2011; Petrik et al. 2013). In contrast to electronic instruments, towed-net collections of plankton allow higher taxonomic resolution, but lower spatial resolution. Automated methods exist to analyze preserved zooplankton samples (e.g., Sieracki et al. 1998; Davis et al. 2005), including the ZooScan benchtop system (Grosjean et al. 2004). The ZooScan system collects digital images of particles larger than a size threshold (usually 0.3 mm) that are processed using computer vision tools to classify zooplankton organisms automatically into taxonomic and size groups (Gorsky et al. 2010). Schultes and Lopes (2009) argued that the combined use of LOPC and ZooScan has the potential to improve our knowledge about how physical factors influence changes in the size spectra, diversity, and energy flow of plankton communities. These instruments are frequently part of contemporary sampling programs.

In order to combine the strengths of the two sampling methods, we have developed an analytical tool combining the high spatial resolution of the LOPC and the taxonomic resolution of net samples analyzed with the ZooScan system to estimate the vertical distributions of multiple zooplankton taxa. The starting point of our analysis was a search for correlations between LOPC size distributions (particle abundances over 42 size classes) and both abundance and size distributions of preserved zooplankton samples analyzed with the ZooScan. We then developed multiple linear regression models between LOPC size classes and dominant zooplankton taxa. We have been able to estimate the vertical distribution of the dominant zooplankton taxa in the water column using the combination of LOPC and net zooplankton data. This technique can provide additional information on zooplankton vertical distribution whenever the LOPC and laboratory-based imaging devices are used in combination. It can also be used to analyze historical data when OPC and LOPC profiles were collected along with net zooplankton samples that can be processed with the ZooScan or other bench top imaging devices.

Materials and methods

Sampling strategy

The data sets contain particle size observations from two instruments: (1) an LOPC 660 (Rolls-Royce), with a detection range of 0.1–35 mm equivalent spherical diameter (ESD), coupled to an interoperable Micro-CTD (AML Microsystems), and (2) a ZooScan system with a 0.3-mm size threshold, which brings the detection range to 0.3–~35 mm ESD. Our study relied on data and samples acquired during three research projects carried out on Brazilian waters (Fig. 1).

Peregrino project

The Peregrino project generated information about the spatial distribution of abundance and size structure for seston and zooplankton on the outer Southeastern Brazilian Continental Shelf (SBCS). The SBCS is under the seasonal influence of the cold and nutrient-rich South Atlantic Central Water (SACW). SACW bottom intrusions over the shelf are driven by changes in wind speed direction and usually occur from late spring through summer. Stronger winds and cold fronts during later autumn and winter tend to erode the pycnocline, increasing vertical mixing and establishing a subsidence setting, referred to here as the TW/CW (Tropical Water/Coastal Water) domain. Sampling was conducted on the Peregrino field during a cruise in April 2010 onboard the RV "Atlântico Sul" over the outer SBCS, off Cabo Frio, Rio de Janeiro. Samples were collected during daytime at 24 stations (Fig. 1a) around two oil platforms before drilling operations began. The LOPC was towed vertically from 10 m above the bottom, which was located at ~100 m depth, to the surface. The plankton net with 200-μm mesh was towed immediately thereafter in the same depth range.

Antares project

The Antares project provided data on mesozooplankton temporal variability during a 5-year time series at a fixed station (23°36′S, 44°58′W) at a 40-m bottom depth on the inner portion of the SBCS off Ubatuba (Fig. 1b). Samples were collected monthly from July 2007 to June 2012 during daylight. This is a region affected by the seasonal interplay of SACW and TW/CW influences (Marcolin et al. 2015).

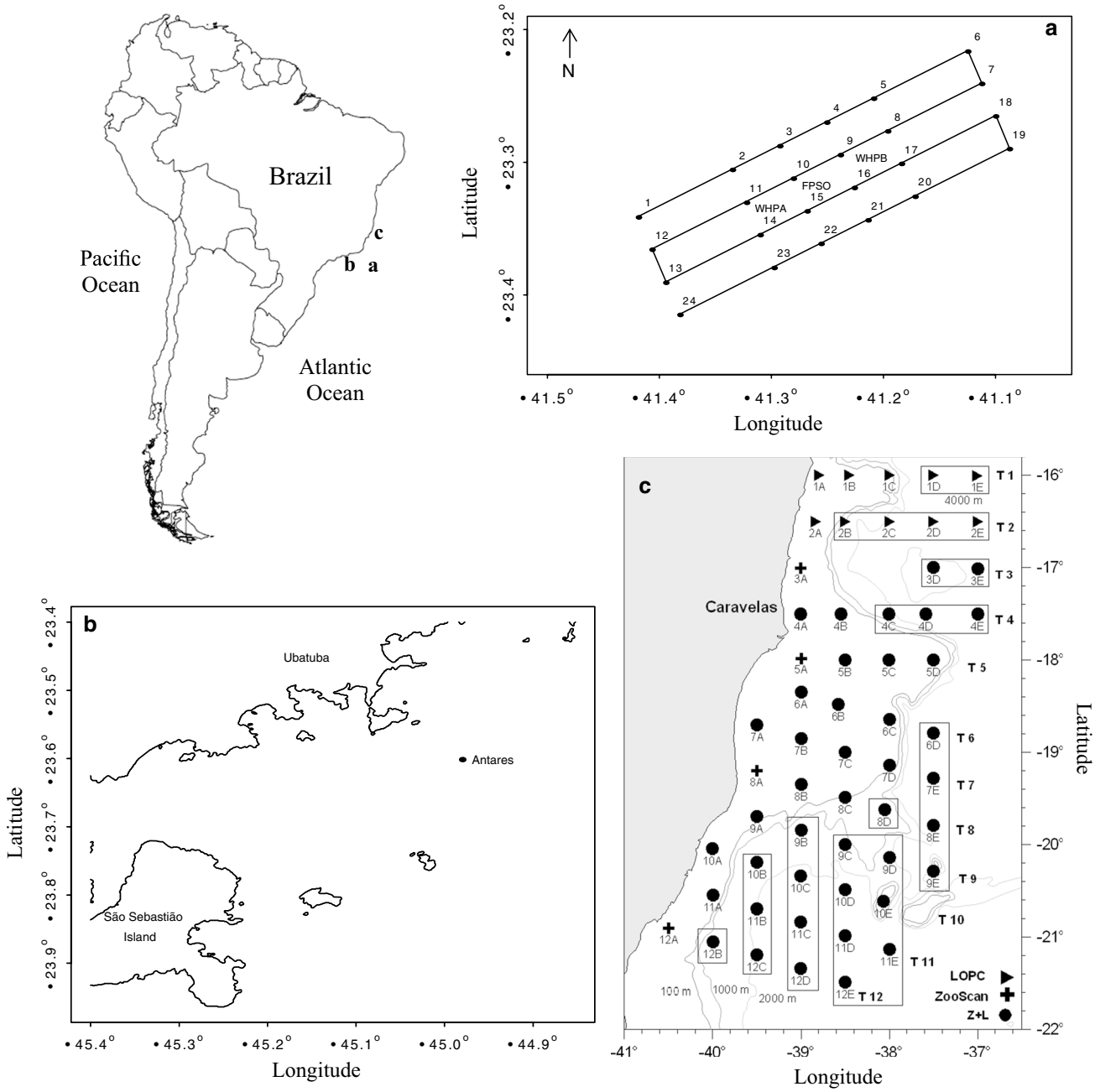

Fig. 1 Study area. **a** Sampling stations on the Peregrino field. **b** Fixed station of the Antares program, off Ubatuba, São Paulo. **c** Sampling stations over the Abrolhos Bank and vicinities; *squares* indicate oceanic stations

The LOPC/Micro-CTD package was towed vertically from 2 to 3 m above the bottom to the surface. The 200-μm mesh plankton nets were towed vertically immediately after LOPC sampling. The water column was sampled in two layers, below and above the thermocline if one was present and below and above the mid-depth otherwise (Marcolin et al. 2015). The two samples were summed for this study to make them comparable to the single samples collected as part of the other two studies.

ProAbrolhos project

The ProAbrolhos project analyzed the spatial distribution of abundance and size structure of seston and zooplankton along the eastern Brazilian coast around the Abrolhos Bank. The ProAbrolhos winter expedition (July–August 2007) sampled an array of 56 stations (Fig. 1c), during both day and night. Local depth varied from 19 to 4000 m. The LOPC/CTD system was installed inside a

conical–cylindrical, 200-μm mesh-sized ring net and was towed vertically as in the Peregrino project. However, tows at deeper stations were limited to a maximum depth of 200 m.

Processing of CTD and chlorophyll fluorescence data

The squared Brunt–Väisällä frequency N^2 was calculated as a measure of the density gradient, from salinity, temperature, and depth measurements, using the SEAWATER toolbox written for MATLAB® (Morgan 1994). In the Antares project, vertical profiles of chlorophyll fluorescence were obtained from a Free-Falling Optical Profiler or Profiler II (Satlantic: http://satlantic.com/profiler). In the ProAbrolhos project, fluorescence was measured with a calibrated fluorometer deployed coupled to a CTD (both from Falmouth Scientific Inc.). No fluorescence data were collected in the Peregrino project.

Sample treatment and image analysis

Analysis of net samples

Net-collected zooplankton samples were preserved in 4 % seawater-diluted formalin, buffered with borax. Each preserved plankton sample was sieved through a 40-μm mesh to remove formalin and resuspended in distilled water. In the Peregrino and Antares projects, each sample was wet-sieved through a 500-μm mesh, and then separate aliquots for organisms <500 and >500 μm were taken to provide better estimates of larger organisms, whereas in the ProAbrolhos project one aliquot was taken per sample using a Motoda splitter (Omori and Ikeda 1984). Aliquots ranged between 1/2 and 1/128 of the whole sample; each aliquot was poured on the ZooScan sample holder and organisms touching each other or close to frame edges were manually separated to avoid overlapping animals before the scanning procedure. Overlapping organisms comprised <10 % of a sample.

We used the Biotom ZooScan model and the latest version of the Zooprocess software at the time of analysis. Zooprocess is a specific ImageJ plugin (http://rsb.info.nih.gov/ij/) developed for plankton image analysis. The ZooScan image resolution was set to 2400 dpi, providing a 16-bit digital image. The average number of particles detected was 1650 particles per scanned image. When the samples contained an excess of detritus, we scanned an additional aliquot to ensure an appropriate number of counted organisms, independent of the non-living particles. The resulting image was normalized, and the raw image was converted to full grayscale range and analyzed with the Plankton Identifier software (Gorsky et al. 2010). A blank background image composed of distilled water was captured and processed every four scanned samples.

A training set was built by sorting 200–300 image vignettes into the desired taxonomic groups (Online Resource 1, Table S1), including categories for detritus, fibers, and carcasses. Different training sets were built for each data set, when applicable. The random forest algorithm with features recommended by Gorsky et al. (2010) was used in the classification step. All samples were manually validated by a taxonomist, who moved the misclassified vignettes to the correct folder, using XnView and Zooprocess to correct errors in the automatic classification. Training set classification errors were typically <25 % for each taxonomic category before validation. The size parameters were converted from pixels to micrometers using the ratio 1.0 pixel: 10.58 μm, consistent with the scanner resolution (Grosjean et al. 2004).

LOPC

The LOPC records objects passing through a 7 × 7 cm cross section of a laser sheet, assigning ESDs to particles based on their light absorption (Herman et al. 2004). We processed the LOPC data into particle size spectra (Herman et al. 2004; Checkley et al. 2008) for each vertical profile at 5-m depth intervals. The depth-integrated particle counts were used to calculate the number spectrum n_T, which is the rate of change in the total particle concentration as size increases (Jackson and Checkley, 2011). We divided the size range of 107 μm to 2.73 cm into 42 size classes, in which the diameter d of the upper bound of each size class was 1.1447 times the diameter of the lower bound. For ΔN objects (number of particles per volume unit) in a small size interval Δd, we approximate, $n_T \approx \frac{\Delta N}{\Delta d}$, as in Jackson and Checkley (2011) and Petrik et al. (2013). We separated aggregates from zooplankton by fitting a normal curve to the peak of the particle volume distribution (nVd) to isolate the distribution of aggregate particles—n_a (Petrik et al. 2013).

The residual distribution (n_z) is the difference between total (n_T) and aggregate (n_a) distributions, $n_z = n_T - n_a$. It is considered to be the zooplankton distribution (Petrik et al. 2013). Using these procedures, we calculated profiles of size distribution for non-living particles (*a*-particles, i.e., particles believed to be aggregates) and zooplankton (*Zo*-particles, i.e., particles within the residual distribution), in addition to the total (*T*-particles). Note that the *Zo*-particles are distinct from the "z-particles" described by Jackson and Checkley (2011), since different methods were used to calculate them. We compared the abundance and size distributions of taxa obtained with the ZooScan with the number of particles within a size range using the residual distribution from LOPC profiles ($\Delta N = n_z \cdot \Delta d$). We also computed

the total aggregate mass distributions, assuming that the particle density equaled 1 mg mm^{-3} (Herman and Harvey, 2006).

We used the same size classes for the ZooScan data as for the LOPC to calculate zooplankton size distributions. These are reported here in the size range where both instruments overlap, corresponding to LOPC classes 9–42 (315 μm–2.7 cm).

Data analysis

We used MATLAB® statistical routines to analyze the count data. The abundance (organisms m^{-3}) estimated for the main taxonomic groups identified in the ZooScan system (hereafter referred to as "zooplankton abundance"), the volumes sampled by the plankton nets, and the volumes sampled by the LOPC for the different data sets can be found as supplementary material (Online resource 1).

Correlating concentrations

We calculated the square of the Pearson's correlation coefficient of determination r^2 and the associated p values using MATLAB®'s *corr* function to compare zooplankton abundances in different size ranges from the ZooScan analysis and from the LOPC *Zo*-particle measurements. Although both the LOPC and ZooScan report sizes as ESD, they measure different physical properties that can result in different reported values for the same particle (e.g., Jackson et al. 1997; Checkley et al. 2008). Because we expected differences between ESD estimates from LOPC and ZooScan, we tested using the feret diameter, the longest distance between any two points along the object boundary (Gorsky et al. 2010), as well as the ESD, for the ZooScan animals. The feret diameter provided a higher number of significant correlations with the LOPC ESD size distributions than did the ZooScan ESD. We also calculated the correlations between zooplankton abundance independent of size and the *Zo*-particle size distributions.

We only considered as reliable the significant correlations ($p < 0.05$) with $r^2 \geq 0.30$, slopes close to 1, and counts >0 at more than 10 stations. We discarded correlations when size ranges differed two times or more from each other (see Online Resource 2), or when concentrations of organisms and particles under comparison were more than an order of magnitude different from each other.

Removing outliers

We performed a principal component analysis (PCA) using the ZooScan-derived size distribution of the main zooplankton taxa to search for samples having zooplankton size distributions excessively departing from the average. According to Hodge and Austin (2004), the PCA is an ideal exploratory analysis to select a subset of attributes in multidimensional data sets. The PCA identifies the principal components containing the greatest variance while preserving maximum information and retaining minimal redundancy. As the principal component scores contain the necessary information to detect the main variability trends from multidimensional data sets, they also provide the means to identify outliers. The most commonly used procedure to detect and eliminate outliers is based on the mean and standard deviation (Selst and Jolicoeur 1994). Consistent with this, we removed the samples with scores outside the range of the mean ± one standard deviation of the second principal component, which contained the largest variability (see the Online Resource 3).

Multiple linear model (MLM)

After excluding outliers, we ran the MATLAB® function *LinearModel.stepwise* to identify which *Zo*-particle size classes were linearly correlated with zooplankton abundance. This function creates a linear regression model by stepwise regression. A constant term (intercept) was not included, and the criterion used to add or remove terms was the p value for an F test of the change in the summed squared error (sse) caused by adding or removing the term. The resulting linear model describes how zooplankton abundance is related to the *Zo*-particle size distribution. The resulting significant relationships were employed to describe vertical distributions of taxonomic groups from LOPC observations.

The influence of sample size on MLM

To evaluate the influence of the number of samples, after removing the outliers (see section "Removing outliers"), we calculated multiple linear regressions to associate zooplankton and *Zo*-particle abundances for random subsamples of the total suite. From the full sample suite of 87 samples, we calculated the multiple regression on 20 different random subsamples of $n = 43$ and 20 subsamples of $n = 66$, as well as the full sample suite of $n = 87$ (50, 75, and 100 % of the total samples, respectively).

Evaluating the MLM

To evaluate further the efficiency of the regressions, we tested whether the fitting procedure worked better for some sets of samples. To do this, we used the relationships determined using a randomly selected subsample ($n = 66$; 75 % of total) to estimate the integrated plankton abundances for all 87 stations, including those not considered in the multiple linear regression analysis. These results were,

in turn, applied in the calculation of normalized residuals [(*observed—estimated*)/*observed*], where *observed* were zooplankton abundances and *estimated* were calculated from the *Zo*-particle size distributions. Then, we displayed the distribution of normalized residuals over all 87 samples.

Results

Zooplankton and particle size distributions: correlations

There were several significant correlations between zooplankton and *Zo*-particle abundances in closely matching size classes, both for the different data sets and for the data set containing data from all three projects (hereafter referred to as PAP data set; Table 1). Most of the significant correlations were for calanoids, poecilostomatoids, decapods, amphipods, and euphausiids (the latter three hereafter referred to as shrimp-like organisms), in the *Zo*-particle size range of 812 μm to ~1.5 mm and 620 μm to ~1.5 mm. Feret diameters of scanned images were usually equal to or larger than the associated *Zo*-particle ESDs.

Zooplankton abundance and LOPC residual size distribution: correlations

Because several size classes of the same zooplankton taxon were correlated with multiple *Zo*-particle size classes (Table 1), we examined the relationships between the total zooplankton abundance, regardless of size, and the *Zo*-particle size distributions. There were significant correlations between the abundances of calanoids, poecilostomatoids, shrimp-like organisms, and appendicularians and the abundances of multiple *Zo*-particle size classes (Table 2). Many of the significant correlations between LOPC and ZooScan size classes were for sizes close to the corresponding taxon size distribution peak (Fig. 2).

The number of significant correlations decreased when all data were considered together. For the PAP data set, only calanoids correlated with *Zo*-particles (Table 2, Fig. 3).

The influence of sample size using the MLM

There were marginally smaller values for R^2 and p when a larger fraction of samples were used to develop the *MLM*; standard deviations for the ensemble of calculations were also lower (Tables 3, 4). The decrease in p is consistent with the increase in sample number. The decrease in R^2 values with increasing number of samples may result from greater variability associated with more samples. However, this decrease may just be a statistical fluke, as the values of R^2 for $n = 87$ are within one standard deviation of the means for the subsamples.

Relating particle and zooplankton distributions using a multiple linear model

There were more significant correlations between the total zooplankton abundance and *Zo*-particle size distributions for the individual sampling programs than there were for the merged PAP data set (Table 2). This difference illustrates the greater variability associated with the increased spatial and temporal range of the combined samples. The outlier removal procedure using PCA was able to compensate for some of the intrinsic variability of zooplankton distributions, as shown by more significant correlations in the PAP data set after the outliers were removed (data not shown). In addition, after the outlier removal procedure, the p values were much smaller for correlations in the combined data than for the three separate projects.

Multiple linear models were able to relate zooplankton abundance and *Zo*-particle size distributions for the PAP data set. Several significant results described the relationship between the abundance of different zooplankton taxa, such as calanoids, poecilostomatoids, shrimp-like shaped organisms, cladocerans, and appendicularians, and different *Zo*-particle size classes (Table 4). Calanoids had the best fit with *Zo*-particles in four separated size ranges, 361–413, 620–710, 1597–1828, and 3139–3594 μm size classes ($R^2 = 0.54$), followed by poecilostomatoids that had a fit to *Zo*-particles ranging from 361–413, 620–710, 1597–1820, and 3139–3594 μm with a slightly smaller relationship ($R^2 = 0.51$). The *MLM* coefficients varied from 0.02 to 30.43 and were greatest for the *Zo*-particle size classes larger than ~1.5 mm; note that LOPC counts were also more similar to zooplankton abundances in these larger size classes when compared to smaller size classes.

Evaluating the multiple linear model

The normalized residuals from the multiple linear model were generally similar for all samples, with a few exceptions, particularly for shrimp-like organisms in the Peregrino project. There was no apparent bias for the 25 % of the samples not used to calculate the regressions so that they could be used as test set (referred as "Test" in Fig. 4). However, the normalized residuals were skewed toward negative values, indicating that LOPC (*Zo*-particles) estimates were systematically higher than the ZooScan-derived estimates. Such bias is also evident when comparing the average size distribution of *Zo*-particles and net plankton data from each project (Fig. 2). *Zo*-particle abundances were usually greater in the size classes correlated with net plankton abundances. The exception was in the Antares

Table 1 Comparisons between concentrations from zooplankton taxa by size classes estimated from scanned images (ZooScan) and Zo-particles abundance by size class (LOPC)

Data set	Zooplankton taxa	Size class range (μm)		Pearson's		*p* value
		ZooScan	Zo-particles	r^2	n_n	
Peregrino $n = 24$	Calanoida	812–930	710–812	0.34	24	3×10^{-3}
	Poecilostomatoida	812–930	710–812	0.44	24	4×10^{-4}
	Poecilostomatoida	812–930	812–930	0.31	24	5×10^{-3}
	Poecilostomatoida	930–1065	710–812	0.43	24	5×10^{-4}
	Poecilostomatoida	1597–1828	620–710	0.36	20	2×10^{-3}
	Poecilostomatoida	1597–1828	710–812	0.38	20	1×10^{-3}
	Poecilostomatoida	1597–1828	812–930	0.36	20	2×10^{-3}
	Shrimp-like	2395–2742	1828–2093	0.32	17	5×10^{-4}
	Ostracoda	812–930	620–710	0.45	18	3×10^{-4}
	Ostracoda	1219–1395	812–930	0.34	11	3×10^{-3}
	Appendicularia	930–1065	710–812	0.41	22	7×10^{-4}
Antares $n = 33$	Calanoida	710–812	620–710	0.36	33	3×10^{-4}
	Calanoida	812–930	620–710	0.41	33	6×10^{-5}
	Calanoida	930–1065	620–710	0.45	33	2×10^{-5}
	Calanoida	1065–1219	620–710	0.41	33	6×10^{-5}
	Calanoida	1219–1395	620–710	0.39	33	1×10^{-4}
	Calanoida	1395–1597	620–710	0.30	33	9×10^{-4}
	Shrimp-like	1828–2093	1828–2093	0.44	33	1×10^{-5}
	Shrimp-like	4113–4708	4113–4708	0.54	11	2×10^{-5}
	Appendicularia	710–812	361–413	0.32	20	6×10^{-5}
	Appendicularia	3593–4113	1828–2093	0.40	16	8×10^{-6}
ProAbrolhos $n = 42$	Calanoida	812–930	620–710	0.33	42	1×10^{-5}
	Calanoida	1219–1395	1219–1395	0.34	40	6×10^{-5}
	Calanoida	1597–1828	1219–1395	0.51	39	2×10^{-7}
	Calanoida	1597–1828	1395–1597	0.46	39	9×10^{-7}
	Calanoida	1597–1828	1597–1828	0.42	39	4×10^{-6}
	Poecilostomatoida	710–812	473–542	0.35	42	4×10^{-5}
	Poecilostomatoida	710–812	542–620	0.30	42	2×10^{-4}
	Shrimp-like	1219–1395	930–1065	0.43	19	3×10^{-6}
	Shrimp-like	1219–1395	1065–1219	0.48	19	4×10^{-7}
	Shrimp-like	1219–1395	1219–1395	0.51	19	1×10^{-7}
	Shrimp-like	1395–1597	1395–1597	0.46	16	8×10^{-7}
	Appendicularia	1828–2093	710–812	0.32	38	1×10^{-4}
	Appendicularia	2093–2395	1219–1395	0.32	40	9×10^{-5}
PAP $n = 99$	Calanoida	620–710	620–710	0.40	97	2×10^{-12}
	Calanoida	620–710	710–812	0.35	97	2×10^{-10}
	Calanoida	710–812	620–710	0.50	99	2×10^{-16}
	Calanoida	710–812	710–812	0.36	99	6×10^{-11}
	Calanoida	812–930	620–710	0.49	99	5×10^{-16}
	Calanoida	812–930	710–812	0.36	99	5×10^{-11}
	Calanoida	930–1065	620–710	0.55	99	2×10^{-18}
	Calanoida	930–1065	710–812	0.41	99	1×10^{-12}
	Calanoida	1065–1219	710–812	0.34	99	1×10^{-13}
	Shrimp-like	4708–5390	4113–4708	0.60	25	8×10^{-21}
	Shrimp-like	4708–5390	4708–5390	0.54	25	4×10^{-18}
	Shrimp-like	5390–6170	5390–6170	0.40	20	2×10^{-12}

Only significant correlations (p values < 0.05) are shown from the Peregrino ($n = 24$), Antares ($n = 21$), and ProAbrolhos ($n = 42$) data sets, and all data sets combined (PAP, $n = 99$); n_n indicates the number of stations with nonzero abundances of organisms estimated with the ZooScan. Note that these correlations were between individual size classes

Table 2 Pearson's r^2 and p values from the significant correlations between ZooScan-derived abundance for different zooplankton taxa and Zo-particle abundance by size class (LOPC) in the three data sets, and with all data sets combined (PAP); n_n indicates the number of stations with nonzero abundances of organisms estimated with the ZooScan

Data set	Zooplankton taxa	Zo-particle size class range (μm)	Pearson's r^2	n_n	p value
Peregrino $n = 24$	Poecilostomatoida	710–812	0.42	24	6×10^{-4}
	Poecilostomatoida	812–930	0.26	24	1×10^{-2}
	Shrimp-like	710–812	0.30	3	5×10^{-3}
	Shrimp-like	1828–2093	0.34	9	3×10^{-3}
	Appendicularia	710–812	0.31	21	5×10^{-3}
Antares $n = 33$	Calanoida	620–710	0.42	33	4×10^{-5}
	Calanoida	710–812	0.31	33	9×10^{-4}
ProAbrolhos $n = 42$	Calanoida	620–710	0.36	40	3×10^{-5}
	Calanoida	1065–1219	0.32	42	1×10^{-4}
	Calanoida	1219–1395	0.35	40	4×10^{-5}
	Shrimp-like	1065–1219	0.55	26	2×10^{-8}
	Shrimp-like	1219–1395	0.56	19	1×10^{-8}
	Shrimp-like	1395–1597	0.60	16	2×10^{-9}
	Appendicularia	1219–1395	0.37	34	2×10^{-5}
	Appendicularia	1597–1828	0.33	37	6×10^{-5}
PAP $n = 99$	Calanoida	620–710	0.55	97	3×10^{-18}
	Calanoida	710–812	0.43	99	2×10^{-13}

data set, where calanoids were more abundant than the *Zo*-particles in the 1065–1219 μm size class, but not in 620–710 μm size class.

Estimating zooplankton vertical distribution using the multiple linear model

The final step in our analyses was applying the significant multiple linear models to estimate the vertical distribution of zooplankton taxa (Table 4), which included calanoids, poecilostomatoids, shrimp-like organisms, and appendicularians.

On the Peregrino field area, calanoids had peaks at ~20, 40, and 90 m depth, whereas poecilostomatoids had a vertical distribution similar to that of aggregates (Fig. 5), peaking mostly at the pycnocline (region with largest N^2). Shrimp-like organisms and appendicularians usually had lower concentrations through the water column, with maxima in deeper waters.

The seasonal variability in the estimated zooplankton vertical distributions was evident in the Antares project data set. During seasonal SACW intrusions (Fig. 6), chlorophyll fluorescence usually was greatest at 20 m depth, above the pycnocline, whereas calanoids had several peaks from 20 to 30 m depth and poecilostomatoids had higher concentrations almost in phase with the calanoid peaks. During the TW/CW phase, both N^2 and chlorophyll fluorescence were evenly distributed in the water column and aggregate concentration increased with depth, presumably because of particle resuspension from the bottom. Calanoids and poecilostomatoids were more abundant below 20 m depth during the TW/CW phase. Shrimp-like organisms were evenly distributed through the water column regardless of the season, whereas appendicularians had peaks near the surface and below 20 m depth in both seasons (Fig. 6).

For the ProAbrolhos project, the average zooplankton vertical distribution was different in the shallow stations over the Abrolhos Bank than at oceanic stations (Fig. 1c). On the shelf, aggregates were more abundant between 20 and 40 m depth (Fig. 7a) and chlorophyll fluorescence was greatest at 20 and 60 m depth. N^2 peaks were closer to the bottom over the shelf, but did not form a distinct pycnocline (Fig. 7); at oceanic stations, both aggregate and chlorophyll concentrations were higher above the pycnocline and decreased with depth (Fig. 7b). At the shelf stations, the average calanoid abundance was highest between ~20 and ~40 m, decreasing with depth; at the oceanic stations, calanoids had peaks near surface, ~40, 60, and ~150 m depth. Poecilostomatoid distributions had several peaks at shelf stations, mostly in the upper 35 m, and peaks at ~50 and ~70 m depth at oceanic stations. Shrimp-like organisms were more abundant between 20 and 30 m depth on the shelf, whereas at oceanic stations, they had more peaks near surface and at ~30 and ~60 m depth. Appendicularians had an abundance peak at ~30–50 m depth over the shelf, while the abundances at oceanic stations were highest above ~80 m depth (Fig. 7c–h).

The general distribution pattern over all data sets was that the most abundant organisms, particles, and chlorophyll fluorescence had higher concentrations above or within the pycnocline, when it was detectable. There were significant ($p < 0.05$) linear correlations between the estimated distribution of zooplankton taxa and the distributions

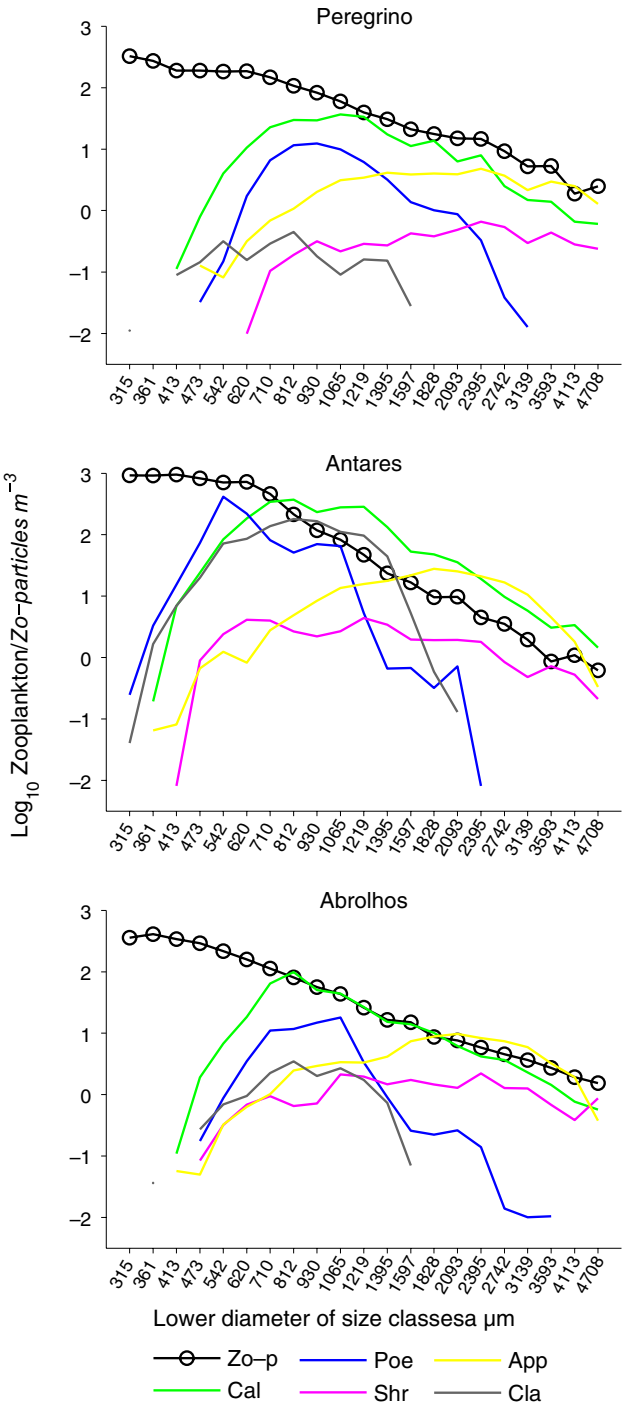

Fig. 2 Size distribution of zooplankton (organisms m^{-3}) and *Zo*-particles (m^{-3}) in the Peregrino field, off Ubatuba (Antares) and over the Abrolhos Bank and vicinities. Values are average of all samples per project. Note the log scale

of aggregates, chlorophyll fluorescence, and N^2 in certain oceanographic settings (Table 5).

Under oligotrophic conditions, poecilostomatoids were more strongly correlated with aggregates and chlorophyll fluorescence (Table 5). There was no significant correlation

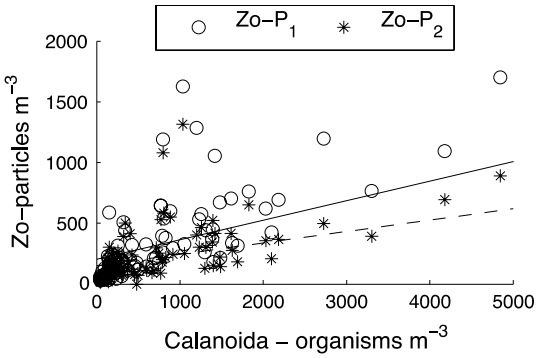

Fig. 3 Correlation between Calanoida abundance and Zo-particle size abundance. All data sets combined (PAP; $n = 99$). Zo-P_1: Zo-particles ranging from 620 to 710 µm; Zo-P_2: Zo-particles ranging from 710 to 812 µm. Pearson's r^2, p values and n are shown in Table 2

between poecilostomatoids and aggregates during SACW intrusions. The value of R^2 was smallest at the Abrolhos Shelf stations. A similar trend was observed for calanoids and appendicularians. When used the PAP data set, there were strong correlations between calanoids, poecilostomatoids, shrimp-like organisms, and appendicularians with both aggregates and N^2. Among the environmental variables, there were also significant correlations between N^2 and aggregates, N^2 and chlorophyll fluorescence, and between fluorescence and aggregates (Table 6).

Discussion

Methodological aspects

By first removing the aggregate contribution from the LOPC size distributions, we were able to improve the correlations between zooplankton abundance estimated from net samples and the particle concentration by size classes estimated with the LOPC. The largest correlations were between the most abundant and widely distributed ZooScan/zooplankton taxa and *Zo*-particles. Although there were also significant correlations ($p < 0.05$, $r^2 > 0.30$) between zooplankton and both aggregate and total particles, they were fewer relative to those with *Zo*-particles (see Online Resource 4). The size classes for the latter set of significant correlations were usually very different than those with the *Zo*-particles, with the correlating diameters often more than twice those for the *Zo*-particles. The zooplankton size classes that correlated with aggregate and total particles belonged mostly to the largest particles, which have fewer counts, implying that the corresponding plankton abundance was zero for most stations (Online Resource 4, numbers in bold characters). Given that the *Zo*-particles are contained within the total particle

Table 3 Results from multiple linear models (*MLM*) using 20 different random subsamples of $n = 43$ and 20 subsamples of $n = 66$ (50 and 75 % of total samples, respectively), after outliers removal

	$n = 43$		$n = 66$	
	R^2	p value	R^2	p value
	Mean ± SD	Mean ± SD	Mean ± SD	Mean ± SD
Calanoida	0.61 ± 0.09	$1 \times 10^{-11} \pm 5 \times 10^{-11}$	0.57 ± 0.08	$2 \times 10^{-17} \pm 4 \times 10^{-17}$
Poecilostomatoida	0.54 ± 0.09	$8 \times 10^{-10} \pm 2 \times 10^{-9}$	0.53 ± 0.06	$3 \times 10^{-15} \pm 6 \times 10^{-15}$
Shrimp-like	0.57 ± 0.14	$8 \times 10^{-9} \pm 2 \times 10^{-8}$	0.49 ± 0.06	$3 \times 10^{-13} \pm 9 \times 10^{-13}$
Appendicularia	0.44 ± 0.16	$6 \times 10^{-7} \pm 2 \times 10^{-6}$	0.37 ± 0.08	$3 \times 10^{-10} \pm 9 \times 10^{-10}$
Cladocera	0.55 ± 0.20	$8 \times 10^{-6} \pm 2 \times 10^{-5}$	0.48 ± 0.10	$1 \times 10^{-7} \pm 7 \times 10^{-7}$

Table 4 Results from linear model fits applied to ZooScan-derived abundance for different zooplankton taxa and Zo-particle concentration by size class, based on the PAP data set ($n = 87$)

Zooplankton taxa	R^2	Linear predictor
Calanoida	0.54	$y_{est} = 0.20 \cdot x_{361–413} + 1.10 \cdot x_{620–710} + 11.57 \cdot x_{1597–1828} - 30.43 \cdot x_{3139–3594}$
p values		$x_{361–413}$: 1×10^{-2}; $x_{620–710}$: 6×10^{-12}; $x_{1597–1828}$: 1×10^{-5}; $x_{3139–3594}$: 3×10^{-5}
Poecilostomatoida	0.51	$y_{est} = 0.80 \cdot x_{315–361} + 0.41 \cdot x_{620–710} - 4.79 \cdot x_{3139–3594}$
p values		$x_{315–361}$: 6×10^{-3}; $x_{620–710}$: 1×10^{-12}; $x_{3139–3594}$: 4×10^{-2}
Shrimp-like	0.45	$y_{est} = 0.02 \cdot x_{361–413} + 0.02 \cdot x_{541–620} + 0.5 \cdot x_{1597–1828} - 0.33 \cdot x_{2092–2394}$
p values		$x_{361–413}$: 5×10^{-5}; $x_{541–620}$: 4×10^{-4}; $x_{1597–182}$: 2×10^{-4}; $x_{2092–2394}$: 2×10^{-2}
Appendicularia	0.36	$y_{est} = 0.19 \cdot x_{620–710} + 3.46 \cdot x_{1597–1828} - 6.70 \cdot x_{3139–3594}$
p values		$x_{620–710}$: 5×10^{-8}; $x_{1597–1828}$: 1×10^{-5}; $x_{3139–3594}$: 1×10^{-3}

Only significant results are shown. y_{est}: estimated plankton vertical distribution; x_i: Zo-particle vertical abundance in the size range (μm) shown in the subscripts

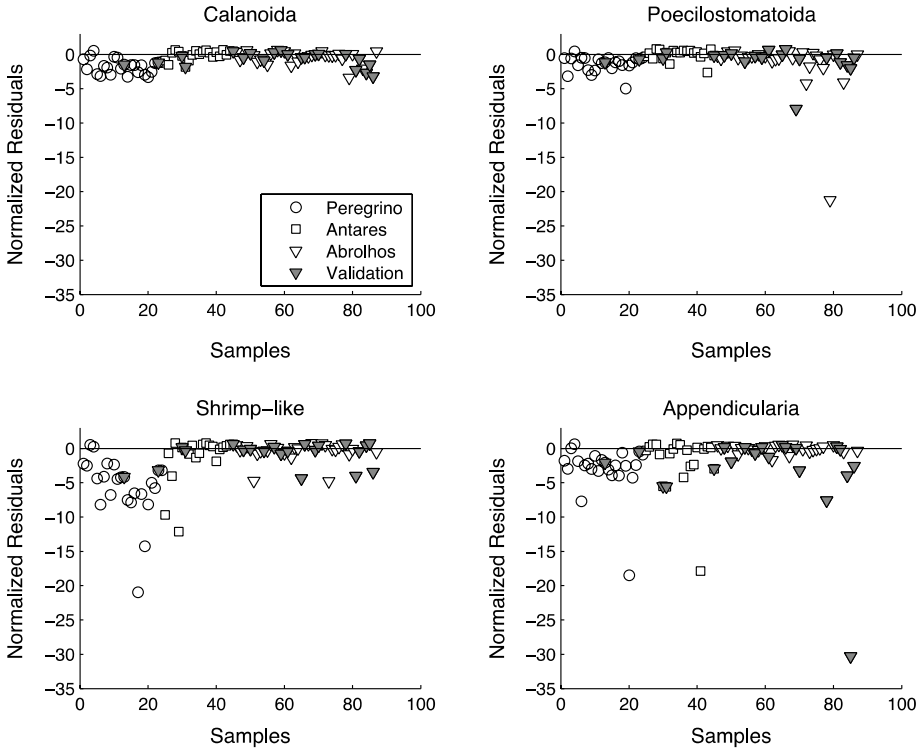

Fig. 4 Normalized residuals [(Observed–Estimated)/Observed] from the multiple linear model. Observed: ZooScan abundances for a given zooplankton taxon (Calanoida, Poecilostomatoida, shrimp-like organisms, and Appendicularia); Estimated: calculated from the LOPC size distributions using the regression coefficients. Symbols indicate samples from different data sets, and "Validation" indicates samples that were not used to build the model

distributions, some correlations should be expected. However, the separation between *Zo*-particles (LOPC residuals) and aggregates provides more realistic estimates of both zooplankton and aggregate size distributions than do the total particles, as was also observed by Petrik et al. (2013). The abundance estimates obtained from LOPC *Zo*-particles

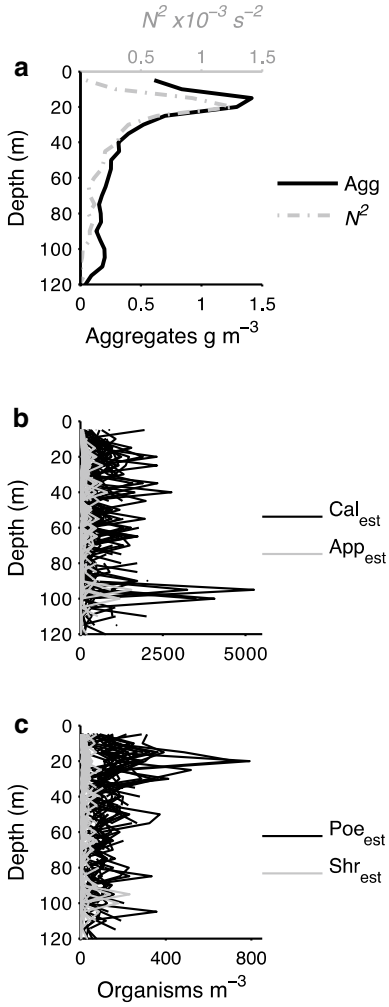

Fig. 5 Vertical profiles of the Brunt–Väisälä frequency (N^2 10^{-3} s^{-2}) and aggregate concentration (g m^{-3}) (a; average), and the estimated plankton abundance (b and c; all samples are shown) in the Peregrino field. Cal_{est}: Calanoida; Poe_{est}: Poecilostomatoida; Shr_{est}: Shrimp-like; App_{est}: Appendicularia; Agg: aggregates, i.e., LOPC particles that fit to a Gaussian distribution

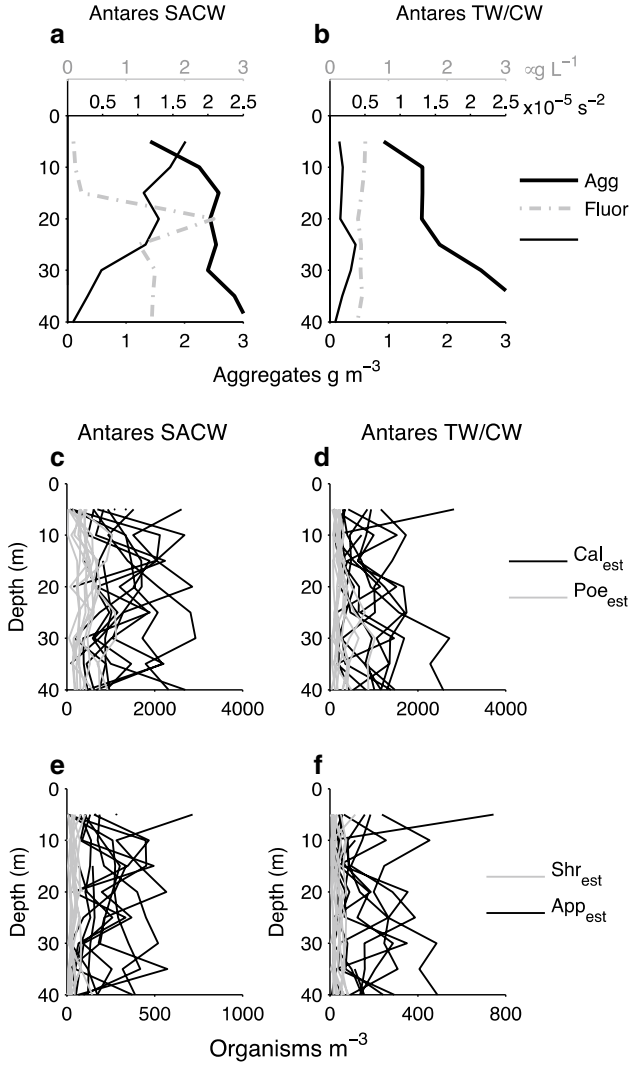

Fig. 6 Vertical profiles of the Brunt–Väisälä frequency (N^2 10^{-5} s^{-2}), aggregate concentration (g m^{-3}), and chlorophyll fluorescence (μg L^{-1}) (**a** and **b**; average), and the estimated plankton abundance (**c**–**f**; all samples are shown) in the Antares fixed station. Left plots show samples during SACW bottom intrusions, whereas right plots show the TW/CW domain. Note different scales of plankton abundances. Cal_{est}: Calanoida; Poe_{est}: Poecilostomatoida; Shr_{est}: Shrimp-like; App_{est}: Appendicularia; Fluor: chlorophyll fluorescence; Agg: aggregates, i.e., LOPC particles that fit to a Gaussian distribution

and ZooScan images were similar, although skewed toward larger abundances with the LOPC. These may reflect the underestimation of the 200-μm net for small organisms since the 200-μm net only samples efficiently the zooplankton in sizes ranging between 450 and 1400 μm (Hopcroft et al. 2001), whereas the LOPC reports particle counts as small as about 100 μm (Herman et al. 2004). For instance, significant numbers of poecilostomatoids can escape such nets since their size abundance peak was at the size range of 542–620 μm in the Antares samples. Note that size distributions of the zooplankton groups decrease dramatically below about 400 μm for the ZooScan samples but not for the *Zo*-particles (Fig. 2).

Most significant correlations considered as reliable (i.e., with $p < 0.05$, $r^2 \geq 0.30$, slopes close to 1, and counts >0 at more than 10 stations), were present among particles/organisms within larger size classes (up to 2.6 times higher, 1.4 times, on average) in the ZooScan than in the LOPC size distributions. These results indicate that the LOPC systematically assigns smaller lengths to the organisms than the ZooScan. Variability in size estimates from the LOPC and the ZooScan is expected for a number of reasons. First, there are different metrics under consideration, and the instruments have different strategies to measure size (Herman et al. 2004; Gorsky et al. 2010). The feret (longest length) measurements used by the ZooScan system are

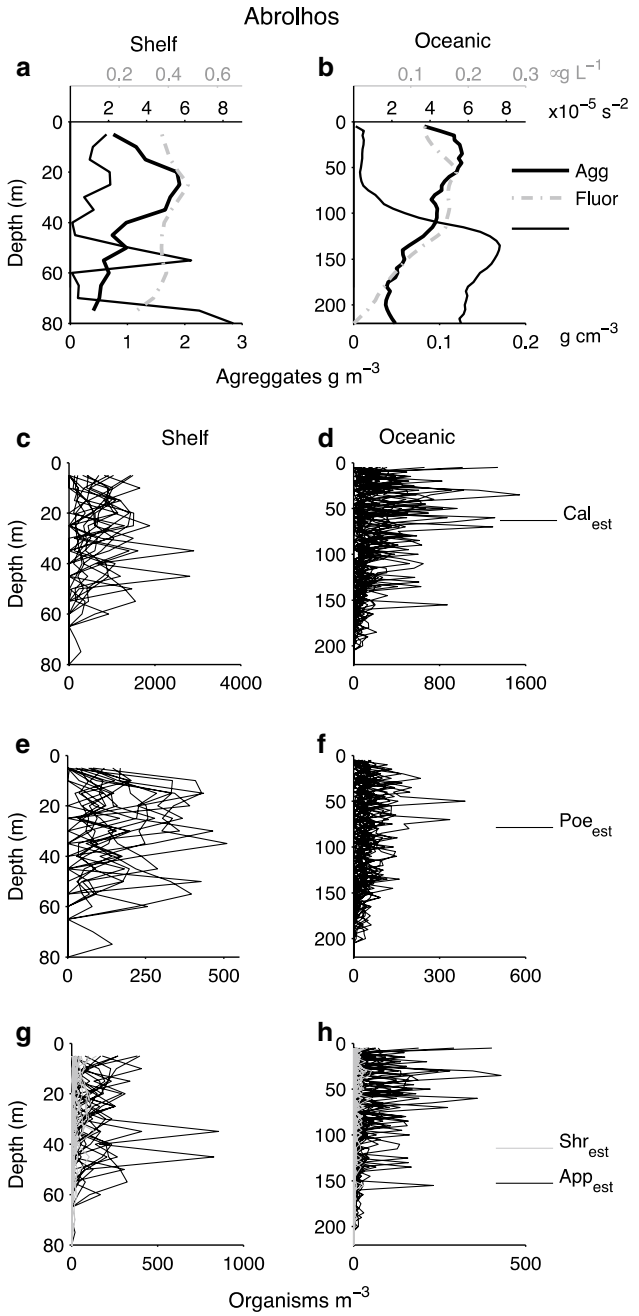

Fig. 7 Vertical profiles of the Brunt–Väisälä frequency (N^2 10^{-5} s^{-2}), aggregate concentration (g m^{-3}), and chlorophyll fluorescence (μg L^{-1}) (**a** and **b**; average), and the estimated plankton abundance (**c**–**h**; all samples are shown) in the Abrolhos Bank and vicinities. Left plots show the average of samples over the shelf domain, whereas right plots show the average of the oceanic domain. Note different scales of plankton abundances. Cal_{est}: Calanoida; Poe_{est}: Poecilostomatoida; Shr_{est}: Shrimp-like; App_{est}: Appendicularia; Fluor: chlorophyll fluorescence; Agg: aggregates, i.e., LOPC particles that fit to a Gaussian distribution

larger than the conserved mass diameter reported by the LOPC (Herman et al. 2004; Basedow et al. 2013). This is because of the non-compact nature of most zooplankton with long bodies, which would yield greater feret lengths than the diameters calculated from their actual volumes (from LOPC). The LOPC reports the ESD taking into account that the particle/organism has the shape of a sphere, which has the smallest feret length for a given volume. It is also important to consider the discontinuity of the size classes from *Zo*-particles that correlated with the ZooScan abundance data. These different size classes could represent populations of organisms from distinct age groups or different species from the distinct oceanographic settings considered in this study.

The individual Zo-particle size classes having the largest correlations with zooplankton taxa were similar in size to the ZooScan distribution peaks. When we analyzed the entire (PAP) data set, the only significant correlations were for highly abundant zooplankton groups. Such correlations provided *p* values orders of magnitude smaller, and the size range was more consistent with zooplankton size distribution peaks when compared to the correlations found for each project separately. When we analyzed the PAP data after removing outlier stations, there were more correlations between the abundance of the most abundant groups, such as poecilostomatoids, cladocerans and appendicularians and *Zo*-particles.

Another relevant methodological consideration comes from Herman et al. (2004), who reported that many large-sized organisms may occlude only a fraction—e.g., 15–40 %—of the LOPC light beam relative to their size, and this has been attributed to their transparent nature. In our study, this could explain why appendicularians were correlated with *Zo*-particle size classes usually ~50 % smaller than the size range measured by the ZooScan for this taxon (see Table 1).

Finally, one should not expect a total agreement in estimates from net samples and LOPC tows because of the additional issue of sampling reproducibility in the patchy ocean environment. Patchiness has always bedeviled sampling programs, so that even two nets towed together in a Bongo configuration will not provide the same results (e.g., Wiebe and Holland 1968). The correlations between zooplankton and *Zo*-particle abundances would certainly improve if natural patchiness could be removed, which is obviously unattainable.

The limited resolution provided by its relatively few channels makes the LOPC inherently unable to generate unique identification of the many species present in the ZooScan data set. This was made possible with the multiple linear regression technique applied here, which will be more efficient when species diversity is not extremely high and under more strict geographic settings and temporal variability. In other words, in less-diversified ecosystems where few species dominate in a particular size range, combining net samples analyzed by ZooScan with

Table 5 Results from linear regression adjustments applied to plankton distributions and environmental variables; N^2: Brunt–Väisällä frequency

Data set	Zooplankton taxa	*n*	Parameter	Oceanographic setting	R^2	*p* value
Peregrino	Poecilostomatoida	24	Aggregates	Outer Shelf off Cabo Frio	0.83	1×10^{-10}
		24	N^2		0.85	2×10^{-11}
Antares	Calanoida	10	Aggregates	TW/CW	0.88	2×10^{-5}
		10	N^2		0.46	5×10^{-2}
	Poecilostomatoida	10	Aggregates		0.92	5×10^{-5}
		10	Fluor		0.61	2×10^{-2}
	Appendicularia	10	Aggregates		0.64	1×10^{-2}
Abrolhos	Calanoida	17	Aggregates	Shelf	0.32	4×10^{-2}
		25	Aggregates	Oceanic	0.66	2×10^{-10}
		17	Fluor	Shelf	0.42	1×10^{-2}
		25	Fluor	Oceanic	0.50	3×10^{-7}
		25	N^2	Oceanic	0.65	3×10^{-10}
	Poecilostomatoida	17	Aggregates	Shelf	0.33	3×10^{-2}
		25	Aggregates	Oceanic	0.74	1×10^{-12}
		25	Fluor	Oceanic	0.69	3×10^{-11}
		25	N^2	Oceanic	0.44	4×10^{-6}
	Shrimp-like	17	Aggregates	Shelf	0.61	5×10^{-5}
		25	Aggregates	Oceanic	0.53	1×10^{-7}
		17	Fluor	Shelf	0.58	1×10^{-3}
		25	Fluor	Oceanic	0.38	2×10^{-5}
		25	N^2	Oceanic	0.59	7×10^{-9}
	Appendicularia	25	Aggregates	Oceanic	0.52	1×10^{-7}
		25	Fluor	Oceanic	0.36	5×10^{-5}
		17	N^2	Shelf	0.39	2×10^{-2}
		25	N^2	Oceanic	0.60	5×10^{-9}
PAP	Calanoida	87	Aggregates		0.79	1×10^{-14}
			N^2		0.48	8×10^{-7}
	Poecilostomatoida	87	Aggregates		0.93	9×10^{-24}
			N^2		0.69	4×10^{-11}
	Shrimp-like	87	Aggregates		0.74	8×10^{-13}
			N^2		0.43	5×10^{-6}
	Appendicularia	87	Aggregates		0.61	2×10^{-9}
			N^2		0.33	1×10^{-5}

Only significant results are shown ($p < 0.05$). No chlorophyll fluorescence data are available for the Peregrino data set. Cal: Calanoida; Poe: Poecilostomatoida; Shr: Shrimp-like; App: Appendicularia. Fluor: chlorophyll fluorescence; TW/CW: Tropical Water and Coastal Water domain; SACW: South Atlantic Central Water domain; Shelf: coastal and shallow stations on the Abrolhos Bank; Oceanic: Deeper stations off Abrolhos Bank vicinities; *n*: number of samples

LOPC tows provides a highly reliable tool to estimate zooplankton vertical distribution with higher taxonomic accuracy and spatial resolution than neither method can provide alone. The ability of the *MLM* parameters calculated with a subset (75 %) of samples to accurately estimate the abundances of the *Test* samples—i.e., the 25 % of samples that were not used in the analyses—shows that these fits have predictive value. The techniques developed here must be tested before being used with other in situ imaging devices.

Plankton and particle distributions

The accumulation of particles and phytoplankton (measured as chlorophyll fluorescence) at and above the pycnocline, as observed for the Antares and Abrolhos stations, is a well-known feature of stratified coastal and oceanic regions (Lampitt et al. 1993; MacIntyre et al. 1995; Sullivan et al. 2010). However, the association between the distribution of zooplankton and aggregates is still not well documented worldwide.

Table 6 Correlations between environmental values

Correlations between environmental variables					
Data set	*n*	Parameters	Oceanographic setting	R^2	*p* value
Peregrino	24	$N^2 \times$ Agg	Outer Shelf off Cabo Frio	0.81	4×10^{-10}
Antares	11	$N^2 \times$ Agg	SACW	0.65	2×10^{-2}
	10	$N^2 \times$ Agg	TW/CW	0.53	3×10^{-3}
Abrolhos	17	Fluor × Agg	Shelf	0.76	3×10^{-5}
	25	Fluor × Agg	Oceanic	0.69	4×10^{-11}
	25	$N^2 \times$ Agg	Oceanic	0.64	7×10^{-10}
	25	$N^2 \times$ Fluor	Oceanic	0.40	9×10^{-6}
PAP	87	$N^2 \times$ Agg		0.69	2×10^{-11}

Only significant values are shown

Agg aggregates, *Fluor* chlorophyll fluorescence

Our novel analytical tool matching LOPC and ZooScan-derived estimates has provided information on the vertical distribution of dominant zooplankton in different marine ecosystems off Brazil. A major finding was that calanoids, appendicularians, and, especially, poecilostomatoids—including oncaeids and corycaeids—are more strongly associated with aggregate-rich layers during oligotrophic conditions, such as at the oceanic sites off Abrolhos or during subsidence phases in the nearshore Antares station. Uye et al. (2002) reported similar trends in the case of the harpacticoid *Microsetella norvegica*, which attaches to marine snow to obtain food in a relatively oligotrophic environment and may live as a free swimmer when suspended particles are abundant. Our results are also consistent with other observations relating an increase in zooplankton abundance to availability of aggregates as a major food source (Alldredge 1972; Paffenhöfer 1983; Green and Dagg 1997; Shanks and Walters 1997; Koski et al. 2005).

Zooplankton feeding has an important influence on particle repackaging (Roullier et al. 2014). Therefore, the coincident peaks in vertical distributions of zooplankton and aggregates observed here imply that marine snow concentration and size may be controlled by the zooplankton feeding pressure in our study sites, thus affecting the aggregate sinking flux (Jackson and Checkley 2011; Jackson et al. 2015). As a result, we expect lower particle export rates under oligotrophic regimes off Brazil relative to those in more productive coastal waters, largely as a result of the vertical connectivity between zooplankton and aggregates.

This study shows the importance of obtaining accurate information about zooplankton vertical distribution within relevant spatial scales. The combined LOPC–ZooScan approach reported here can be readily implemented in many sites worldwide both as a standalone technique and as a companion to in situ imaging devices. In either case, the application may assist to improve our understanding of several key aspects of marine ecosystems dynamics, such as the role of zooplankton aggregations as a major food resource for small pelagic fish, and the implications of zooplankton feeding to the biological pump.

Concluding remarks

We developed a technique incorporating the high spatial resolution of the LOPC and the ZooScan taxonomical information to estimate the vertical distribution of abundant mesozooplankton taxa. Peaks of zooplankton and aggregate concentration usually coincided with each other and with the pycnocline, particularly in oceanic and coastal sites influenced by tropical oligotrophic waters. Although our analytical tool has intrinsic limitations regarding the ZooScan image resolution or the interpretation of size measurements by the different instruments (e.g., two different particles in ZooScan assigned to the same size range in LOPC could indicate two different species, or two different-sized particles within the same species), virtually any comparable instrumentation will suffer from similar drawbacks. For instance, some currently available imaging devices may still provide low counts relative to those determined from net tows (Basedow et al. 2013; Roullier et al. 2014); other sampling methods may not cover relevant segments of the size spectrum, such as small meso- and microzooplankton (Cowen and Guigand 2008), preventing comparisons with the lowest LOPC size range. Nevertheless, we encourage the analysis of historical data whenever both LOPC and plankton net samples were collected together and net samples can be processed using a ZooScan or another imaging device. Such usage of multiple data sources is essential to increase the data availability from different marine ecosystems, which is crucial to improve the predictions of zooplankton vertical distribution based on the multiple regressions proposed here.

Acknowledgments This research is a contribution from the international network ANTARES (www.antares.ws), the ProAbrolhos project (Conselho Nacional de Desenvolvimento Científico e Tecnológico—CNPq—Grant 420219/2005-6 to Eurico C. Oliveira), and the Peregrino project (funded by Statoil). C.R.M. was supported by CNPq (141409/2010-0 and 141793/2012-0, PhD fellowship) and Coordenação de Aperfeiçoamento de Pessoal de Nível Superior (CAPES, BEX 18255/12-4); R.M.L. was supported by the CNPq grant 311936/2013-0 and several additional grants from CAPES, CNPq (including INCT Mar COI), FINEP and FAPESP. We thank the valuable comments of the anonymous reviewers that greatly contributed to improve this manuscript.

References

Alldredge AL (1972) Abandoned larvacean houses: a unique food source in the pelagic environment. Science 177:885–887. doi:10.1126/science.177.4052.885

Basedow SL, Tande KS, Zhou M (2010) Biovolume spectrum theories applied: spatial patterns of trophic levels within a mesozooplankton community at the polar front. J Plankton Res 32:1105–1119. doi:10.1093/plankt/fbp110

Basedow SL, Tande KS, Norrbin MF, Kristiansen SA (2013) Capturing quantitative zooplankton information in the sea: performance test of laser optical plankton counter and video plankton recorder in a Calanus finmarchicus dominated summer situation. Prog Oceanogr 108:72–80. doi:10.1016/j.pocean.2012.10.005

Benfield MC, Grosjean P, Culverhouse PF, Irigoien X, Sieracki ME, Lopez-Urrutia A, Dam HG, Hu Q, Davis CS, Hansen A, Piskaln CH, Riseman EM, Schultz H, Utgoff PE, Gorsky G (2007) RAPID research on automated plankton identification. Oceanography 20:172–187

Calbet A, Landry MR (2004) Phytoplankton growth, microzooplankton grazing, and carbon cycling in marine systems. Limnol Oceanogr 49:51–57. doi:10.4319/lo.2004.49.1.0051

Checkley DM, Davis RE, Herman AW, Jackson GA, Beanlands B, Regier LA (2008) Assessing plankton and other particles in situ with the SOLOPC. Limnol Oceanogr 53:2123–2136

Cowen RK, Guigand CM (2008) In situ ichthyoplankton imaging system (IS IIS): system design and preliminary results. Limnol Oceanogr Methods 6:126–132

Davis CS, Thwaites FT, Gallager SM, Hu Q (2005) A three-axis fast-tow digital Video Plankton Recorder for rapid surveys of plankton taxa and hydrography. Limnol Oceanogr MethodsOceanography methods 3:59–74

Gorsky G, Ohman MD, Picheral M, Gasparini S, Stemmann L, Romagnan J-B, Cawood A, Pesant S, García-Comas C, Prejger F (2010) Digital zooplankton image analysis using the ZooScan integrated system. J Plankton Res 32:285–303. doi:10.1093/plankt/fbp124

Green EP, Dagg MJ (1997) Mesozooplankton associations with medium to large marine snow aggregates in the northern Gulf of Mexico. J Plankton Res 19:435–447. doi:10.1093/plankt/19.4.435

Grosjean P, Picheral M, Warembourg C, Gorsky G (2004) Enumeration, measurement, and identification of net zooplankton samples using the ZOOSCAN digital imaging system. ICES J Mar Sci 61:518–525. doi:10.1016/j.icesjms.2004.03.012

Herman AW, Harvey M (2006) Application of normalized biomass size spectra to laser optical plankton counter net intercomparisons of zooplankton distributions. J Geophys Res 111:1–9. doi:10.1029/2005JC002948

Herman AW, Beanlands B, Phillips EF (2004) The next generation of optical plankton counter: the laser-OPC. J Plankton Res 26:1135–1145

Hodge VJ, Austin J (2004) A survey of outlier detection methodologies. Artif Intell Rev 22:85–126

Jackson GA, Checkley DM (2011) Particle size distributions in the upper 100 m water column and their implications for animal feeding in the plankton. Deep Res Part I 58:283–297. doi:10.1016/j.dsr.2010.12.008

Jackson GA, Maffione R, Costello DK, Alldredge AL, Logan BE, Dam HG (1997) Particle size spectra between 1 mm and 1 cm at Monterey Bay determined using multiple instruments. Deep-Sea Res I 44:1739–1767

Jackson GA, Checkley DM, Dagg M (2015) Settling of particles in the upper 100 m of the ocean detected with autonomous profiling floats off California. Deep Sea Res I 99:75–86. doi:10.1016/j.dsr.2015.02.001

Koski M, Kiørboe T, Takahashi K (2005) Benthic life in the pelagic: aggregate encounter and degradation rates by pelagic harpacticoid copepods. Limnol Oceanogr 50:1254–1263. doi:10.4319/lo.2005.50.4.1254

Lampitt RS, Wishner KF, Turley CM, Angel MV (1993) Marine snow studies in the Northeast Atlantic Ocean: distribution, composition and role as a food source for migrating plankton. Mar Biol 116:689–702

Lopes RM (2007) Marine zooplankton studies in Brazil: a brief evaluation and perspectives. Acad Bras Cienc 79:369–379

MacIntyre S, Alldredge AL, Gotschalk CC (1995) Accumulation of marine snow at density discontinuities in the water column. Limnol Oceanogr 40:449–468

Marcolin CR, Schultes S, Jackson GA, Lopes RM (2013) Plankton and seston size spectra estimated by the LOPC and ZooScan in the Abrolhos Bank ecosystem (SE Atlantic). Cont Shelf Res 70:74–87. doi:10.1016/j.csr.2013.09.022

Marcolin CR, Gaeta S, Lopes RM (2015) Seasonal and interannual variability of zooplankton vertical distribution and biomass size spectra off Ubatuba, Brazil. J Plankton Res 1–12. doi:10.1093/plankt/fbv035

Mitra A, Castellani C, Gentleman WC, Jónasdóttir SH, Flynn KJ, Bode A, Halsband C, Kuhn P, Licandro P, Agersted MD, Calbet A, Lindeque PK, Koppelmann R, Møller EF, Gislason A, Nielsen TG, StJohn M (2014) Bridging the gap between marine biogeochemical and fisheries sciences; configuring the zooplankton link. Prog Oceanogr 129:176–199. doi:10.1016/j.pocean.2014.04.025

Morgan PP (1994) SEAWATER: A library of MATLAB computational routines for the properties of sea water*: Version 1.2*. CSIRO Marine Laboratories

Omori M, Ikeda T (1984) Methods in marine zooplankton ecology. John Wiley and Sons, New York

Paffenhöfer G-A (1983) Vertical zooplankton distribution on the northeastern Florida shelf and its relation to temperature and food abundance. J Plankton Res 5:15–33

Petrik CM, Jackson GA, Checkley DM (2013) Aggregates and their distributions determined from LOPC observations made using an autonomous profiling float. Deep Sea Res Part I Oceanogr Res Pap 74:64–81. doi:10.1016/j.dsr.2012.12.009

Roullier F, Berline L, Guidi L, Sciandra A, Durrieu De Madron X, Picheral M, Pesant S, Stemmann L (2014) Particle size distribution and estimated carbon flux across the Arabian Sea oxygen minimum zone. Biogeosciences 11:4541–4557. doi:10.5194/bg-11-4541-2014

Schultes S, Lopes RM (2009) Laser optical plankton counter and Zooscan intercomparison in tropical and subtropical marine ecosystems. Limnol Oceanogr Methods 7:771–784. doi:10.4319/lom.2009.7.771

Shanks AL, Walters K (1997) Holoplankton, meroplankton, and meiofauna associated with marine Snow. Mar Ecol Prog Ser 156:75–86

Sieracki CK, Sieracki ME, Yentsch CS (1998) An imaging-in-flow system for automated analysis of marine microplankton. Mar Ecol Prog Ser 168:285–296. doi:10.3354/meps168285

Sullivan JM, Donaghay PL, Rines JEB (2010) Coastal thin layer dynamics: consequences to biology and optics. Cont Shelf Res 30:50–65. doi:10.1016/j.csr.2009.07.009

Trudnowska E, Szczucka J, Hoppe L, Boehnke R, Hop H, Blachowiak-Samolyk K (2012) Multidimensional zooplankton observations on the northern West Spitsbergen Shelf. J Mar Syst 98–99:18–25. doi:10.1016/j.jmarsys.2012.03.001

Uye S, Aoto I, Onbé T (2002) Seasonal population dynamics and production of Microsetella norvegica, a widely distributed but little-studied marine planktonic harpacticoid copepod. J Plankton Res 24:143–153

Van Selst M, Jolicoeur P (1994) A solution to the effect of sample size on outlier elimination. Q J Exp Psychol Sect A 47:631–650. doi:10.1080/14640749408401131

Vandromme P, Nogueira E, Huret M, Lopez-Urrutia Á, González-Nuevo González G, Sourisseau M, Petitgas P (2014) Springtime zooplankton size structure over the continental shelf of the Bay of Biscay. Ocean Sci 10:821–835. doi:10.5194/os-10-821-2014

Wiebe PH, Benfield MC (2003) From the Hensen net toward four-dimensional biological oceanography. Prog Oceanogr 56:7–136. doi:10.1016/S0079-6611(02)00140-4

Wiebe PH, Holland WR (1968) Plankton patchiness: effects on repeated net tows. Limnol Oceanogr 13(2):315–321

Yamaguchi A, Matsuno K, Abe Y et al (2014) Seasonal changes in zooplankton abundance, biomass, size structure and dominant copepods in the Oyashio region analysed by an optical plankton counter. Deep Sea Res I 91:115–124. doi:10.1016/j.dsr.2014.06.003